



COB-2021-2070

FATIGUE LIFE PREDICTION OF A STRUCTURE SUBJECTED TO RANDOM LOADS AND STATISTICAL DURABILITY TESTS

Vinicius Lugli

Paulo José Paupitz Gonçalves

School of Engineering, São Paulo State University (UNESP), Bauru, Brazil
vinicius.lugli@unesp.br; paulo.paupitz@unesp.br

Abstract. *One of the most significant challenges for the industry is estimating the fatigue life of products during the design phase, when not all of its components have been finalized and tested. The most widespread methods for structures fatigue life prediction are based on the Rainflow algorithm and time-domain; however, several researches are carried out to improve the efficiency of this process, as well as Dirlik's, which proposes to use the spectral-domain and a PDF. Thus, the main objective of this work is to evaluate two different fatigue life prediction methods through FEA. As a complement, a statistical durability test of the designed structure was developed using a hydraulic shaker. In addition to the durability results, the tests allowed the determination and calibration of structure's parameters that were used as FEA input. Through the FEA calculations and fatigue estimations, we concluded that the Dirlik's method provides more severe fatigue conditions when compared to the Rainflow method, and both processes were less severe than the average results of the durability test. Considering satisfactory results for both processes, the spectral method becomes a feasible solution in determining the fatigue cycle of random and extensive time-history.*

Keywords: *Fatigue life, Power spectral density (PSD), Finite element analysis (FEA), Probability density function (PDF), Dirlik's method*

1. INTRODUCTION

In the design process of a structure subjected to dynamic loads, estimating the fatigue cycle due to dynamic random load is probably one of the most challenging steps. Performing numerical analysis and fatigue life prediction are essential to reduce time and costs of the structure design process.

In the agricultural machinery design process, these difficulties are often present as they are very complex structures, with different machine layout configurations and for their use in different types of terrains. The great motivation to carry out this study is to understand, with help of experimental tests, what is the best cost and benefit among the most used methodologies in the fatigue life prediction of a structure subjected to a random dynamic load.

According to Benasciutti and Tovo (2006), Yoon *et al.* (2015), studies, fatigue life predictions are traditionally performed in the time-domain, using all input signals and numerical model results as a time-history and the fatigue cycle counting performed by Rainflow algorithm, (Lindgren and Rychlik, 1987). Therefore, due to the need of having a complete stress time-history for each structure hot-spot, when using transient dynamic analysis (TDA) it is important to pay attention to very extensive time-history and the complexity of the numerical model. These characteristics bring a practical problem to this numerical analysis.

Another way of predicting fatigue life for a random process is to use the spectral methods, although not trivial. Frequency-domain methods have some advantages over that use of the time-domain, such as the characterization of the structure's behavior due to modal parameters and a greater computational efficiency of the numerical analysis. The fatigue life prediction process in the spectral method, according to Dirlik (1985), is to obtain a stress range PDF from the PSD of the random dynamic fatigue load combined with the structure's FRF.

A recent study by Gadolina *et al.* (2021) discusses the advantages of time and spectral methods in the estimation of fatigue life. To summarize, the authors conclude that the estimation of the durability in the time-domain using the Rainflow cycle counting and corrected linear hypothesis to be superior for robust estimation for all levels of stress of random loading. In practical cases, however, the time-domain computation may be impractical depending on the model's size to be considered. Several studies on frequency-domain methods exist, such as (Braccesi *et al.*, 2015); (Kvittem and Moan, 2015); (Mršnik *et al.*, 2013); (Yoon *et al.*, 2015), where the authors make a fair comparison of various methodologies presented in the literature.

This work compares fatigue estimation results and the results obtained from the durability test performed on a device excited by a hydraulic shaker. The structure designed for the practical bench test will serve as a reference to obtain the material parameters that must be inserted in the FEA and as a statistical validation of the fatigue life prediction results obtained by the Rainflow method. Finally, with the FE model calibrated, an efficiency analysis will be

made between the proposed methods, confronting the FEA computational cost and the difference of the fatigue life prediction results.

2. FATIGUE LIFE PREDICTION PROCESS

The present research aims to analyze the feasibility of different fatigue life prediction processes with the aid of FEA and an empirical model performed on a hydraulic shaker test. As described in the diagrams of both fatigue estimation processes, Figure 1, first it is necessary to define a fatigue load signal, which can be a time-history obtained directly from the structure or by a virtual multibody dynamic model.

Among the methods for fatigue life prediction, those using the time-domain are more conventional and present several advantages and disadvantages. The most significant disadvantages are related to the definition of time-history that represents a complex fatigue cycle and the TDA solution cost. However, when it comes to the spectral method, as proposed by Dirlik (1985), it is possible to estimate the stress range PDF through the structure's stress range FRF combined with the PSD of an extensive fatigue cycle time-history, thus eliminating the Rainflow cycle counting and some expensive steps in the computer simulation process.

The first necessary information in both processes is the fatigue cycle time-history, Figure 1(a-i) and 1(b-i), which were created randomly in a wideband frequency that favors the amplification of structure's dynamic response, with first and second natural frequency modes equal to 17,8 Hz and 44,7 Hz, respectively. Thus, this time-domain signal has been applied as hydraulic shaker input, and this fatigue load was confirmed by the structure's dynamic response acquisition from coupled accelerometers at the specimen end and in the center of the test device, as shown in Figure 2(a), defining the fatigue load sample in the time-domain.

This measured time-history is used in different ways in each process. In the time-domain method, this acceleration signal is an input for the TDA in the FEA model, and in the spectral method, this signal is processed to obtain the fatigue load PSD.

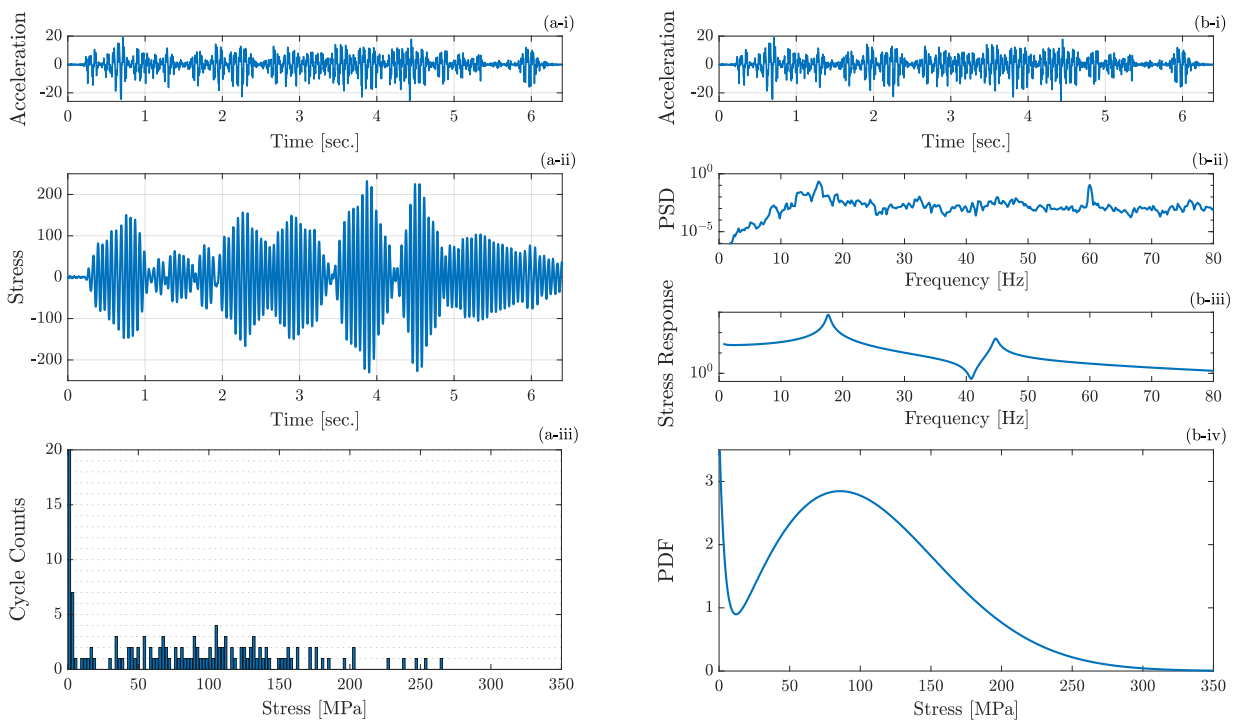


Figure 1. Workflow of fatigue life prediction methods, (a) Time-domain process, (b) Spectral method process (Dirlik).

The output of TDA is a stress time-history, Figure 1(a-ii), which is used by the Rainflow cycle counting algorithm to determine the number of stress range cycles in this signal, Figure 1(a-iii), thus making it possible to estimate the accumulated damage using the theory proposed by Palmgren (1924), Miner (1945). In the spectral method, the PSD of the fatigue load, Figure 1(b-ii), is combined with a stress range FRF, Figure 1(b-iii), obtained from FE harmonic response analysis, and these functions are used by Dirlik's method to calculate the stress range PDF, Figure 1(b-iv), and estimate the accumulated fatigue damage as in the time-domain process.

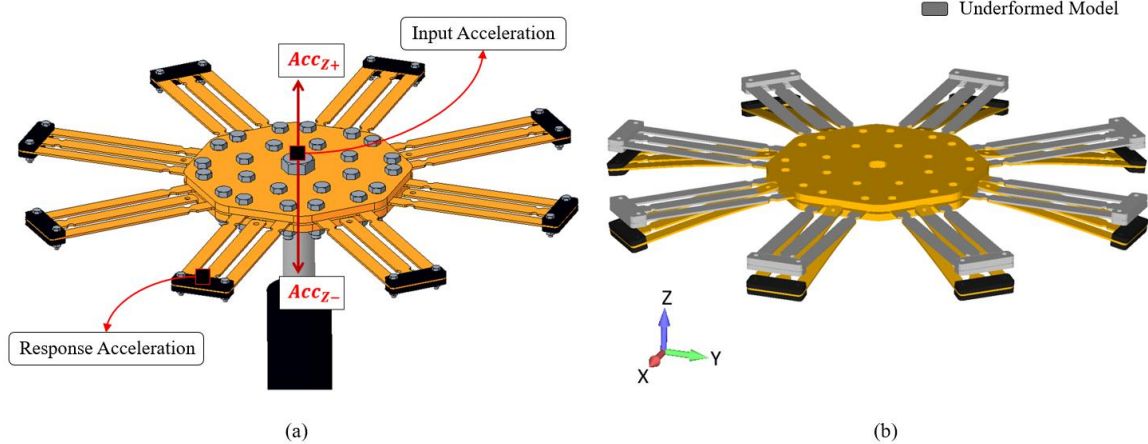


Figure 2. (a) Hydraulic shaker uniaxial actuation direction on the Z-axis. (b) Specimen bending response shape for shaker uniaxial load.

As designed and presented in Figure 2(b), the structure responds to the uniaxial shaker load, Figure 2(a), in a bending shape and, consequently, with tensile and compressive stresses in the specimen hot spot, simplifying the fatigue damage composition.

2.1 Test device design and FEA parameters calibration

During the definition of the characteristics of the structure under analysis and the inputs of the hydraulic shaker, it was found the need to perform a test with accelerated fatigue, create a random input signal for the shaker and reduce as much as possible multiaxial stresses due to the torsion shape. Therefore, to achieve this objective, a structure more susceptible to bending mode with a geometric notch in the hotspot region was designed and detailed below in Figure 3.

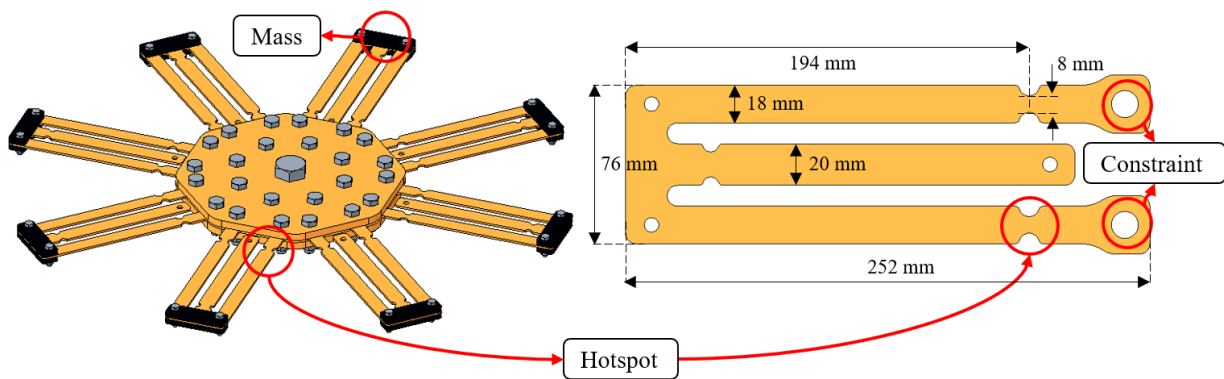


Figure 3. Device assembly and specimen dimensions designed for fatigue testing.

Table 1. Experimental results of mechanical properties for Steel NBR 6656 – LNE 38

Steel Properties ⁽¹⁾	NBR 6656 – LNE 38
Young's Modulus (GPa)	208,0 ± 8,0
Tensile Strength, Yield (MPa)	407,2 ± 10,9
Tensile Strength, Ultimate (MPa)	504,1 ± 9,1
Elongation at Break (%)	27,9 ± 1,2

⁽¹⁾ measured at 25°C

In order to analyze the structural behavior under an axial load is necessary to define the specimen mechanical properties, so that these parameters can be used in a static load analysis using finite element method (FEM). The FEA response is a symmetrical bending shape represented in Figure 2(b) and the stress gradient in Figure 4, which also demonstrates the fulfilment of one of the objectives during the specimen design, which is to avoid the incidence of shear and torsional stresses reducing the influence of multiaxial stresses on the sum of structural damage. The LNE38 -

NBR 6656 Steel was chosen for specimen manufacture, and its mechanical properties, listed in Table 1, are used as FEA model input and to estimate the material fatigue stress strength.

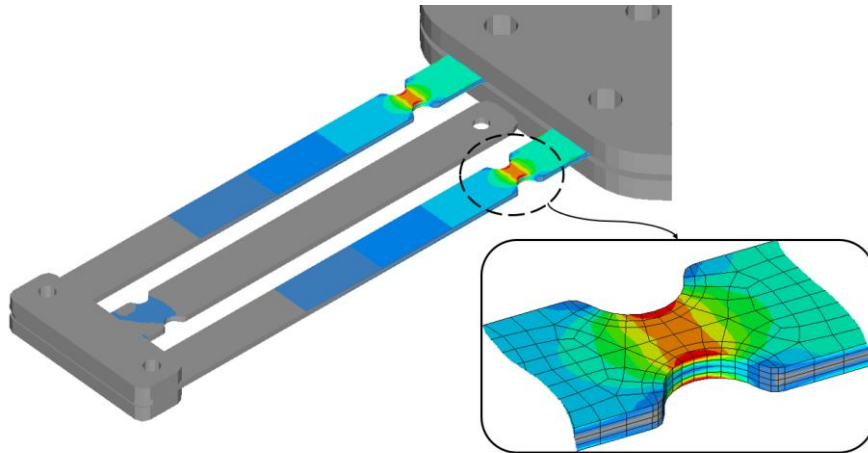


Figure 4. Structure's stress distribution gradient and finite element mesh refinement in the hot spot.

To perform a TDA and a harmonic response analysis, in addition to the data in Table 1, it is necessary to define other material parameters that are decisive for studying the dynamic behavior of the specimen, including material density and structure damping factor. Density can be easily determined and will be used to calculate the mass matrix, the stiffness matrix is calculated from FE type, geometry and the Young's modulus, listed in Table 1, and the damping matrix can be calculated using a global damping factor, viscous damping factor or a proportional (structural) damping factor, which is not trivially obtained when dealing with a structure with several components and vibration modes.

Despite the difficulty in obtaining these parameters, using two accelerometers coupled to the device designed for the test to measure the input and output signal, as shown in Figure 2(a), it is possible to calculate the real transfer function (TF) of the dynamic system and with this information perform the calibration of the structural damping factor, (Garbin, 2015), of the FEM model bringing the computationally simulated response closer to the measured response.

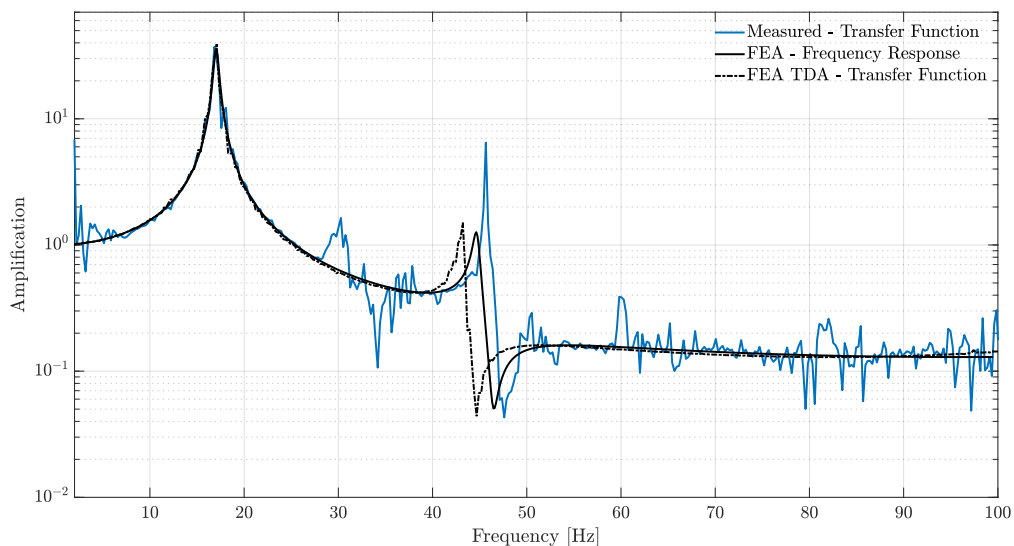


Figure 5. Calibration of FEA dynamic response by the damping factor through comparison with the response measured in a test device.

Through the graph in Figure 5, it is possible to conclude that there is a difference between the TF of the dynamic system obtained by the FRF and TDA responses; despite this difference, both dynamic responses are very similar to the measured TF. The FEA response for the first natural mode, which is the most relevant, is practically coincident with the real one. However, for the second natural mode, despite the similarity between the response amplitudes, it is possible to observe a small deviation in the frequency value that is not related to structural damping factor calibration.

2.2 Miner's rule

The fatigue damage accumulation method chosen for this research is the one proposed by Palmgren (1924) and then developed by Miner (1945), this is a linear damage accumulation theory and, due to its simplicity, is widely used in the structure design process. The damage increment per cycle, according to this method, depends on the combination of load characteristics and stress range cycle count,

$$\frac{dD}{dN} = \frac{1}{N_f(\sigma_a)} \quad (1)$$

where, $N_f(\sigma_a)$ is the number of cycles required for failure under alternating fatigue stress σ_a . This number is obtained from the S-N-P curves of the specimen's material. The S-N curves are composed of the amplitude of the alternating stress and the number of cycles that this structure's material withstands under this stress until fatigue failure.

Considering a fatigue load with alternating stress range σ_{ai} , and the number of cycles until fatigue failure N_{fi} , obtained by the material's S-N curve, it is possible to calculate the accumulated damage after n_i cycles through Eq. (2), and rewriting Eq. (1) to obtain Eq. (3).

$$N_f = k\sigma_a^{-m} \quad (2)$$

where $k = S_f^m$, and S_f is a material fatigue strength limit

$$D_i = \frac{n_i\sigma_a^m}{k} \quad (3)$$

To enable the calculation of accumulated fatigue damage D_i , the number of cycles, n_i , for each stress range, σ_{ai} , in which the structure was subjected, is determined by the stress range cycle counting using the Rainflow method, in case of a time-domain analysis, or by a stress range PDF in fatigue life prediction by the Dirlik's method.

Palmgren-Miner claim in their theory that component fatigue failure occurs when the damage summation is equal to or greater than one, $D_t \geq 1$. This result is obtained by the linear sum of the fractions of damage caused to the structure during its working life.

$$D_t = D_1 + D_2 + \dots + D_n = \sum_{i=1}^n \frac{n_i\sigma_{a,i}^m}{k} \quad (4)$$

One of the caveats made by Zoroufi (2004) about the Palmgren-Miner method concerns the sum of damage fractions regardless of the order of occurrence of stress range cycles. However, the objective of this research does not include the evaluation of the damage accumulation method, but to perform a comparative analysis between different fatigue life prediction methods using the same damage accumulation model. For this reason, the least complex and widely used method in the engineering environment was chosen for this research development.

2.3 Rainflow stress range cycle counting

Components and structures during their working period are subject to cyclical loads, and to account for these cycles it is necessary to decompose this load into stress/strain cycles that are characterized by their average value and amplitude, where the amplitude can be constant or variable throughout time. The Rainflow cycle counting method aims to reduce a complex load with time-varying stress range in a matrix with the number of cycles of constant stress range.

Considering a structure subjected to fatigue cycling with constant amplitude, the accounting of fatigue cycles and their respective amplitudes are done directly, not requiring any complex methodology. In a complex case, where the structure is subjected to random loading with variable amplitudes, the stress response over time will have the same characteristic, making it difficult to identify the cycles and their amplitudes. In order to solve this problem, some techniques have been improved and standardized with the development of several researches and some examples of these techniques are detailed by Lee (2005).

Rainflow algorithm used in this project is based on the four-point cycle counting method, which is also known as the cycle extraction method. This algorithm is applied in a step of four consecutive points in the stress time history, and this is applied for the whole signal to extract the number of cycles for each constant stress range, which can be organized according to the bar graph in Figure 6.

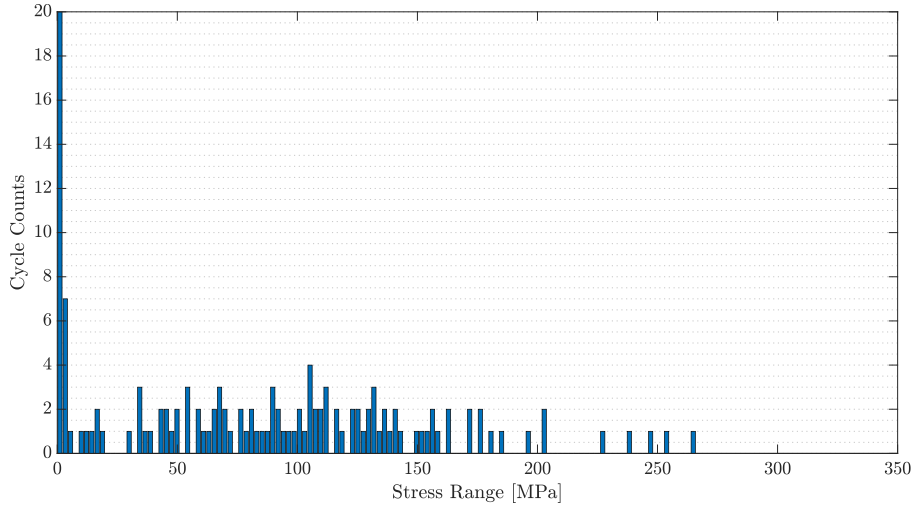


Figure 6. Stress range cycle count by the Rainflow method.

Once the cycle counting matrix has been determined for each stress range, to estimate the durability of the structure, it is necessary to perform the damage accounting during the fatigue process, which will be done using Eq. (4) according to the method proposed by Palmgren (1924) and Miner (1945). During this research, the fatigue stress strength of the specimen's material, S_f , will be used to estimate the failure of the designed structure in the durability test.

2.4 Dirlik's spectral method

The spectral method objective is to avoid the use of extensive signals as fatigue load input. These signals are obtained through several field measurements, test tracks and other situations that represent the work demands of the structure and, by composing these measured signals, it is possible to create a signal that represents the structure's fatigue cycle. Unlike time-domain fatigue estimation methods, which use a time-history as fatigue cycle input, the spectral method uses a PSD of time-history signal to represent the fatigue load cycle.

For these and other difficulties, Dirlik (1985) proposed a methodology that estimates the fatigue cycles through the probability of occurrence of events. The method starts with the determination of the random input signal PSD, that combined with the stress FRF at the hot spot makes it possible to obtain the stress range PDF of random process.

Dirlik's study analyzed the behavior of a Rainflow and a stress range PDF for over 60 processes with different power spectrum characteristics with the help of Monte Carlo simulations. The purpose of this analysis was to enable the application of this method to estimate the stress range PDF for processes with wideband and narrowband frequency. The stress range PDF, as proposed by Dirlik, is calculated by Eq. (5), which is composed of a weighted combination between an exponential function and two Rayleigh distributions and has the probability of occurrence of a stress σ_a in a random process.

$$f(\sigma_a) = p(\sigma_a) = \frac{D_1}{2Q\sqrt{M_0}} e^{-\frac{Z^2 \sigma_a^2}{2R^2}} + \frac{D_2 Z}{2R^2 \sqrt{M_0}} e^{-\frac{Z^2 \sigma_a^2}{2R^2}} + \frac{D_3 Z}{2\sqrt{M_0}} e^{-\frac{Z^2 \sigma_a^2}{2}} \quad (5)$$

The validation of this method was done by computing the different stress range distributions in the time domain by Rainflow cycle counting and fitting a general expression for the PDF based on the 0th, 1st, 2nd and 4th spectral moments, represented by the general equation, as:

$$M_n = (-1)^n \frac{d^n R_X(\tau)}{d\tau^n} = \frac{1}{2\pi} \int_{-\infty}^{\infty} \omega^n S_X(\omega) e^{i\omega\tau} d\omega \quad (6)$$

Considering a broadband random process, the expected up-crossing rate of the random process can be written using the spectral moments, $E[0^+]$, as Eq. (7a), and the expected rate of peak crossing, $E[P]$, as Eq. (7b).

$$E[0^+] = \sqrt{\frac{M_2}{M_0}}; E[P] = \sqrt{\frac{M_4}{M_2}} \quad (7a,b)$$

The empirically determined weighting factors are described as,

$$D_1 = \frac{2(X_m - \gamma^2)}{1 + \gamma^2}; D_2 = \frac{1 - \gamma - D_1 + D_1^2}{1 - R}; D_3 = 1 - (D_1 + D_2);$$

$$Q = \frac{1.25(\gamma - D_3 - D_2R)}{D_1}; R = \frac{\gamma - X_m - D_1^2}{1 - \gamma - D_1 + D_1^2}$$
(8a-e)

The irregularity factor, γ , as explained by Lee (2005), is the ratio of the zero up-crossing rate, Eq. (7a), to the peak crossing rate, Eq. (7b), and can be written, as Eq. (9a). The main frequency of the random signal, X_m , as Eq. (9b) and the normalized stress amplitude, Z , defined by Eq. (9c):

$$\gamma = \frac{M_2}{\sqrt{M_0 M_4}}; X_m = \frac{M_1}{M_0} \sqrt{\frac{M_2}{M_4}}; Z = \frac{1}{2\sqrt{M_0}}$$
(9a-c)

Considering the occurrence probability of stress range $\sigma_{a,i}$, $p(\sigma_{a,i}) = n(\sigma_{a,i})/N_{cycles}$, the damage accumulation model proposed by Dirlik, as a function of a time interval τ , can be written by manipulating the model proposed by Palmgren-Miner, Eq. (4), as shown below.

$$D_t = \frac{E[P]\tau}{k} \sum_{i=1}^n p(\sigma_a) \sigma_{a,i}^m$$
(10)

thus, the number of cycles in τ seconds is given by

$$E[N] = E[P]\tau$$
(11)

According to Ragan and Manuel (2007), on some occasions, it is usual to represent the damage as a function of an equivalent fatigue load (EFL), this is possible by manipulating the Eq. (2).

$$EFL = \sum_{i=1}^n p(\sigma_a) \sigma_{a,i}^m$$
(12)

and replacing Eq. (11) and (12) in Eq. (10), yields

$$D_t = \frac{E[N]}{k} EFL$$
(13)

2.5 Results and discussion

The results can be analyzed in several ways, two of them are absolute fatigue life prediction for each method and a comparison between the EFL prediction, with both forms following the same calculation process. However, the first one requires the material's S-N curve data, while the second form of analysis, as it is comparative, uses only the stress cycles accounted for by Rainflow and the stress PDF estimate and compares the fatigue life cycle predicted by each method.

The results are presented first as an absolute fatigue life prediction, as shown in Table 2, at the end of this session, with a comparative analysis of the computational cost between the two proposed methods and the estimated EFL between the methods and durability test results.

Table 2. Numerical results for fatigue life predicting

Solving Method	Fatigue Life [cycles]	Fatigue Life [h]	FEA - Elapsed Time [h]
Time Domain Method – Rainflow Cycle Counting	80783	22,44	4:21:43
Spectral Method – Dirlik PDF	69247	19,24	1:51:25

The fatigue estimation result for both the TDA and Rainflow cycle counting and for the spectral method and Dirlik's PDF will have a slight divergence with the result of the durability test, Table 3(a), even after the damping factor calibration of the FEA model. This divergence occurs for several reasons, but mainly due to the use of the fatigue stress

strength of NBR 6656 – LNE 38 steel obtained theoretically as proposed by Budynas and Nisbett (2011), and not by the most recommended way that would be to obtain the S-N curve of the material from a standardized fatigue test.

However, to confirm the satisfactory behavior of computational analysis by the FEM and the hot spot fatigue life prediction, Figure 7 represents the repeatability and symmetry of the specimen's failure mode during the first loop of the durability test.



Figure 7. Characteristic of fatigue failures of specimens during the first loop of the durability test.

Table 3(a). Specimen failures during durability tests

Loop 1		Loop 2		Loop 3	
Specimen	Fatigue Life [h]	Specimen	Fatigue Life [h]	Specimen	Fatigue Life [h]
3	9,9	9	10,6	17	8,8
6	13,7	10	13,4	22	13,2
7	16,4	14	14,3	20	15,9
2	17,9	16	15,7	24	17,2
1	18,2	11	18,1	19	17,3
8	20,6	13	20,1	18	18,1
5	21,3	12	21,1	21	19,8
4	22,8	15	24,5	23	21,1

With the experimental results detailed in Table 3(a), it is possible to perform the statistical calibration of the fatigue strength stress, S_f , used in the fatigue life prediction to a value consistent with the average result of the failures of the specimens during the fatigue test, but this is not the main purpose of this paper.

Table 3(b). Statistical parameters of durability test

Number of Specimens	24
Mean Time to Failure	17,08 h
Standard Deviation [SD]	$\pm 4,09$ h
Mean – SD	12,99 h
Mean + SD	21,17 h

To assist in the efficiency analysis of the estimated fatigue results, the graph in Figure 8 compares the average result of the specimen's failure during the endurance test with the fatigue life prediction results. The markers on the graph represent the results of both fatigue life prediction methods, the center line represents the mean value of failure in the durability test, the inner dotted lines represent one process standard deviation, and the outer dotted lines represent two process standard deviations. The statistical variables of the experimental process are detailed in Table 3(b).

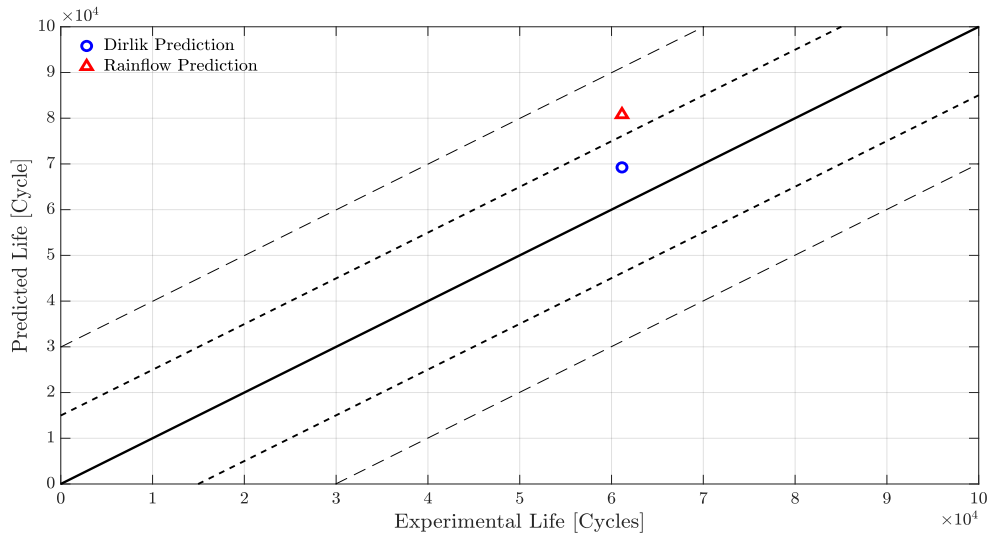


Figure 8. Comparative analysis between durability test results and the fatigue life prediction for the Rainflow and Dirlik's method.

The results contained in Table 4 below consider the average fatigue failure of the specimens during the durability test as a reference and compare it with the results obtained by the fatigue life estimates.

Table 4. Durability test results and fatigue life prediction comparison

Analyzed Method	Fatigue Life [h]	Prediction Error [%]
Experimental Results (mean)	17,08	-
Rainflow Method Prediction	22,44	+12,6%
Dirlik's Method Prediction	19,24	+31,4%

The fatigue life prediction process did not consider the variation of the material's mechanical properties, described in Table 1, since the objective of this research is to compare the results of methods that use the same data and the same material. Thus, the fatigue stress strength value was estimated from the mean value of the material's ultimate stress, $S_{ut} = 504,1 \text{ MPa}$, disregarding its variations, however, the standard deviation of $\pm 9,1 \text{ MPa}$ in the value of S_{ut} would cause a variation of approximately $\pm 23\%$ in the result of fatigue life prediction in both methods.

The variation between the predictions and the experimental result is common, and it occurs because it is not feasible to carry out the shaker load signal acquisition during the whole test period and mainly to use a very extensive time-history as TDA input. As mentioned in the previous items, due to these difficulties, it is common to compose samples of the fatigue load signal to better represent the complete fatigue cycle of the structure.

A summary of the possible influences for the variation of fatigue life estimation results in relation to the experiment can be explained by a deviation in the theoretical estimate of the material fatigue stress strength, variation of material mechanical properties in each specimen, see Table 2, and errors in the FEA model during the determination of material parameters that are used as input properties of the finite element type or in the representation of the whole fatigue cycle by a small sample of a random load, used as TDA input, as it is impractical to use very extensive input signals.

Therefore, considering the discussion of the previous paragraphs and the results contained in Table 4, even if starting from a single measured excitation signal for the two proposed methodologies, a more severe result was obtained by the spectral method due to the fatigue estimation being performed from an event probability function, given by a PDF. The comparison between the fatigue life prediction methods is useful for understanding the characteristics of each method, evaluating the computational cost of different FEA, the quality of fatigue life prediction results and detecting opportunities for improvement in the process of each method to obtain a closer result between them and between the experimental results.

Table 5. Fatigue life prediction methods comparison

Evaluation Parameter	Rainflow	Dirlik
Computational Cost [sec.]	15.703	6.685
Variation to the Experiment [%]	+31,4%	+12,6%
Predictions Ratio (Rainflow/Dirlik) [%]		+16,7%
Costs Ratio (Rainflow/Dirlik) [%]		+234,9%

2.6 Conclusions

The greater difference in the result obtained by the Rainflow method when compared to the Dirlik's result, detailed in Table 5, can be explained by small variations in the fatigue loading applied by the hydraulic shaker during the durability test that was not covered by the excitation sample that was collected by accelerometer. This observation must be considered, as the result of the fatigue life estimate in the time-domain depends on the quality of representation of the total fatigue cycle by a sample of this load that is used as TDA input by the MEF.

One of the advantages of Dirlik's method in comparison to time-domain methods, when it comes to a random fatigue cycle, is the reduction of the error in the complete fatigue cycle estimation due to the statistical representation of the fatigue events. This is only possible because this method uses an event occurrence PDF to estimate the complete fatigue cycle, and this function is calculated through the PSD of complete random load that represents the fatigue load cycle.

If the primary goal of this research was to reduce the fatigue life prediction error due to the determination of the material fatigue stress strength, S_f , it would be recommended to perform a fatigue test on the specimens to obtain the S-N curve of the material. However, the main goal of this research is to obtain the ratio between the computational cost and fatigue life prediction of the different methods to study the feasibility of using the process proposed by Dirlik. Thus, a difference of 16.7% in fatigue life estimation results and a computational cost of approximately 2.35 times lower, comparing frequency response analysis with TDA, make it feasible to use the method of Dirlik for further research.

3. ACKNOWLEDGEMENTS

The authors would like to thank Máquinas Agrícolas Jacto S/A for providing the experimental tests facilities and authorizing the publication of the results.

4. REFERENCES

- Benasciutti, D., & Tovo, R. (2006). Comparison of spectral methods for fatigue analysis of broad-band Gaussian random processes. *Probabilistic Engineering Mechanics*, 21(4), 287–299. <https://doi.org/10.1016/j.probengmech.2005.10.003>
- Braccesi, C., Cianetti, F., & Tomassini, L. (2015). Random fatigue. A new frequency domain criterion for the damage evaluation of mechanical components. *International Journal of Fatigue*, 70, 417–427. <https://doi.org/10.1016/j.ijfatigue.2014.07.005>
- Budynas, R. G., & Nisbett, J. K. (2011). Elementos de Máquinas de Shigley - Projeto de Engenharia Mecânica. <http://mechfamilyhu.net/download/uploads/mech145022803743.pdf>
- Dirlik, T. (1985). *Application of Computers in Fatigue Analysis*.
- Gadolina, I. V., Makhutov, N. A., & Erpalov, A. V. (2021). Varied approaches to loading assessment in fatigue studies. *International Journal of Fatigue*, 144(September 2020), 106035. <https://doi.org/10.1016/j.ijfatigue.2020.106035>
- Garbin, N. L. S. (2015). *Estudo de técnicas para a determinação da matriz de amortecimento em sistemas estruturais*. Universidade Tecnológica Federal do Paraná - campus Pato Branco.
- Kvittem, M. I., & Moan, T. (2015). Frequency versus time domain fatigue analysis of a semisubmersible wind turbine tower. *Journal of Offshore Mechanics and Arctic Engineering*, 137(1), 1–12. <https://doi.org/10.1115/1.4028340>
- Lee, Y. L. (2005). Fatigue Analysis in the Frequency Domain. *Fatigue Testing and Analysis*, 369–394. <https://doi.org/10.1016/B978-075067719-6/50011-7>
- Lindgren, G., & Rychlik, I. (1987). Life Prediction Under Gaussian Load Processes, 10(3), 251–260.
- Miner, M. A. (1945). Cumulative fatigue damage. *Journal of applied mechanics*, 12, 159–164.
- Mršnik, M., Slavič, J., & Boltežar, M. (2013). Frequency-domain methods for a vibration-fatigue-life estimation - Application to real data. *International Journal of Fatigue*, 47, 8–17. <https://doi.org/10.1016/j.ijfatigue.2012.07.005>
- Palmgren, A. G. (1924). Die Lebensdauer von Kugellagern (Life Length of Roller Bearings). *Zeitschrift des Vereins Deutscher Ingenieure*, 68(14), 339–341. <https://doi.org/ISSN 0341-7258>
- Ragan, P., & Manuel, L. (2007). Comparing estimates of wind turbine fatigue loads using time-domain and spectral methods. *Wind Engineering*, 31(2), 83–99. <https://doi.org/10.1260/030952407781494494>
- Yoon, M., Kim, K., Oh, J. E., Lee, S. B., Boo, K., & Kim, H. (2015). The prediction of dynamic fatigue life of multi-axial loaded system. *Journal of Mechanical Science and Technology*, 29(1), 79–83. <https://doi.org/10.1007/s12206-014-1212-1>
- Zoroufi, A. F. A. M. (2004). Fatigue Performance Evaluation of Forged versus Competing Manufacturing Process Technologies : A Comparative Analytical and Experimental Study. *24th Forging Industry Technical Conference, Cleveland, Ohio, 2002*, (September), 286.

5. RESPONSIBILITY NOTICE

The authors are the only responsible for the printed material included in this paper.